



Published in final edited form as:

Magn Reson Med. 2009 April ; 61(4): 810–818. doi:10.1002/mrm.21909.

Postmortem MRI of Human Brain Hemispheres: T_2 Relaxation Times during Formaldehyde Fixation

Robert J. Dawe¹, David A. Bennett², Julie A. Schneider², Sunil K. Vasireddi¹, and Konstantinos Arfanakis¹

¹Department of Biomedical Engineering, Illinois Institute of Technology, Chicago, Illinois, USA

²Rush Alzheimer's Disease Center, Rush University Medical Center, Chicago, Illinois, USA

Abstract

Unlike *in vivo* imaging, postmortem MRI allows for invasive examination of the tissue specimen immediately following the MR scan. However, natural tissue decomposition and chemical fixation cause the postmortem tissue's MRI properties to be different from those found *in vivo*. Moreover, these properties change as postmortem fixation time elapses. The goal of this study was to characterize the T_2 relaxation changes that occur over time in cadaveric human brain hemispheres during fixation. Five hemispheres immersed in formaldehyde solution were scanned on a weekly basis for three months postmortem, and once again at six months postmortem. The T_2 relaxation times were measured throughout the hemispheres. Over time, T_2 values near the edges of the hemispheres decreased rapidly after death, while T_2 values of deep tissue decreased more slowly. This difference is likely due to the relatively large distance from the hemisphere surface, and other barriers limiting diffusion of formaldehyde molecules to deep tissues. In addition, T_2 values in deep tissue did not continuously decay to a plateau, but instead reached a minimum and then increased to a plateau. This final increase may be due to the effects of prolonged tissue decomposition, a hypothesis that is supported by numerical simulations of the fixation process.

Keywords

postmortem; MRI; fixation; T_2

Introduction

For research purposes, postmortem MRI of the human brain offers an advantage over *in vivo* imaging in that a postmortem sample can be sliced for histological examination immediately following the MRI scan (1-13), or otherwise tested in ways that are not appropriate for living subjects (14). However, postmortem imaging of the brain also presents new challenges that have not been dealt with for *in vivo* imaging. In particular, the MRI properties of postmortem tissue can change rapidly as a result of decomposition and chemical fixation. These largely uncharacterized changes in the tissue properties of the postmortem brain can lead to errors in the interpretation of MR findings, and can pose complications in the selection of appropriate data acquisition parameters. The purpose of this work was to investigate the MR-related changes that occur in a human brain hemisphere during formaldehyde fixation.

The goal of chemical fixation is to preserve postmortem tissue in a state similar to that found *in vivo* (15). This can be accomplished by immersing the brain in a solution that contains a fixative agent such as formaldehyde. Over time, the fixative agent diffuses inward from the surface of the brain, slowing or stopping tissue decomposition. However, until complete fixation occurs, postmortem tissue remains vulnerable to bacterial degradation and autolysis (15). Formaldehyde fixation of the tissue promotes protein cross-linking (16-18) and immobilization of water molecules and may lead to a reduction of the T_2 relaxation time (19). Conversely, decomposition of the tissue may lead to increased water content or increased water mobility which may increase T_2 values. Thus, T_2 relaxation can potentially provide important information about the changes that occur in brain tissue during fixation.

Postmortem brain MRI studies have demonstrated that T_2 values are lower in a fixed postmortem brain than *in vivo*, for both white and grey matter (20-23). One investigation indicated that T_2 values at locations near the surface of the brain decreased sharply within the first 7 days of formaldehyde fixation, reaching a plateau after that (up to five weeks postmortem) (20). In another study, three fixed brains were each scanned up to 21 times over the course of three weeks, and it was shown that T_2 values of tissue located within 1.4 cm of the brain surface decreased sharply and reached a plateau within approximately 5 days postmortem (21). In an 11-week-long study, the T_2 values of frontal grey matter in formaldehyde-fixed brains were observed to decrease sharply in the first 10 hours postmortem (22). None of the aforementioned studies explicitly reported on T_2 changes in deep brain tissue, nor have prior studies examined fixed tissue over a period of more than three months.

Sustained T_2 increases in any kind of fixed postmortem tissue have seldom been reported (14,16). In the most recent study to report such a T_2 increase, a small sample of bovine nasal cartilage was immersed for nine weeks in 0.1% formalin (~0.04% formaldehyde) solution (16). During this time, its T_2 value increased significantly by about 12 ms. A similar, though non-significant T_2 increase was observed in a cartilage sample that was immersed in a stronger 1% formalin (~0.4% formaldehyde) solution. Meanwhile, a cartilage sample immersed in 10% formalin (~4% formaldehyde) exhibited a significant T_2 decrease of 40 ms over the same time period. Noting that 0.1% and 1% formalin solutions are relatively weak compared to the 10% formalin solutions commonly used for tissue fixation, it was surmised that the T_2 increases were the result of collagen fibril degradation outpacing the development of formaldehyde-induced collagen cross-links. It was concluded that, in the absence of abundant protein cross-links, the water molecules became relatively mobile within the tissue, leading to elevated T_2 values.

The purpose of the current work was to investigate longitudinally, and for an extended period of time postmortem, T_2 relaxation changes occurring in human brain hemispheres during formaldehyde fixation, and to evaluate the temporal behavior of these changes in brain tissue near the surface of the hemisphere, as well as in deep tissue. To this end, MRI scans of five human brain hemispheres were conducted weekly for a period of three months postmortem, with a follow-up scan for each hemisphere at six months postmortem. T_2 values were measured throughout the hemispheres at each time point. Numerical simulations were also carried out in order to demonstrate how a fixative agent may alter T_2 as it diffuses into the hemisphere. To our knowledge, this is the first longitudinal study to measure T_2 relaxation times throughout cadaveric brain hemispheres for such an extended period of time.

Methods

Experiments

Brain Hemisphere Preparation—The same procedure was used to prepare cerebral hemispheres from five subjects who had consented to donate their brain tissue for research as part of longitudinal clinical-pathologic studies of aging (24). After removing the calvarium and dura mater, the autopsy technician extracted 20 milliliters of cerebrospinal fluid from the ventricular system using an 18-gauge needle and syringe. Next, the cranial nerves were severed. The spinal cord was severed as distally as possible within the spinal canal. Immediately following removal of each intact brain, the cerebrum was separated from the cerebellum and brainstem by cutting through the cerebral peduncles rostral to the mammillary bodies. The cerebrum itself was then divided into left and right hemispheres by bisecting the corpus callosum. One hemisphere was immersed in phosphate-buffered 4% formaldehyde solution (prepared from paraformaldehyde) and refrigerated at 4° C within 30 minutes after removal from the skull. The time between death of the subject and immersion of the hemisphere in solution (postmortem interval, PMI) averaged 4 hours and 35 minutes for the five hemispheres used in this study. The side of the brain from which the hemisphere was removed, the postmortem interval, the age at death, and the sex of each subject are listed in Table 1.

Image Acquisition—Prior to the first MR imaging session, the hemispheres were removed from refrigeration in order for them to reach room temperature. Each hemisphere was re-submerged in a plastic container filled with 4% formaldehyde, with the exposed midsagittal plane of the hemisphere resting on the bottom of the container. Tight-fitting lids were placed on the containers to limit the loss of solution due to evaporation. A wooden bridge-like apparatus, shown in Fig. 1, was constructed in order to reduce the transmission of vibrations from the MRI scanner to the hemispheres during the high spatial resolution scans. The entire apparatus contained no metal and made no direct contact with the scanner.

All scans were performed using a 3.0-T GE MRI scanner (General Electric, Waukesha, WI). A 2D fast spin echo sequence was used to acquire proton density weighted (PD-weighted) and T_2 -weighted images, in sagittal slices through the hemispheres, using the following parameters: TR = 3.6 s, TE₁ = 13.0 ms, TE₂ = 52.0 ms, echo-train length = 6, FOV = 16 × 16 cm, slice thickness = 1.5 mm, acquisition matrix = 256 × 256 zero-padded to 512 × 512, NEX = 6. The total scan time was 31 minutes. Each brain hemisphere was imaged weekly for approximately three months, with the first scan occurring within the first two weeks after death. Each brain also underwent a single follow-up scan at six months postmortem. The temperature of the solution was monitored during each scan session to ensure minimal deviation from ambient room temperature. In the time between scan sessions, the samples were stored in their plastic containers, at room temperature. For each hemisphere, the formaldehyde solution was changed either once or twice prior to the first scan, depending on how long the hemisphere was stored in refrigeration before being scanned. Approximately 24 hours prior to the first scan, the solution was changed again. The formaldehyde solution in each container was changed four times throughout the scanning period.

Post-processing—The PD-weighted and T_2 -weighted images were used to calculate the T_2 relaxation time on a voxel-by-voxel basis according to the mono-exponential decay model $S_2 = S_1 \exp(-t/T_2)$, where S_1 and S_2 are the signal intensities at TE₁ and TE₂, respectively, and $t = TE_2 - TE_1$. Maps of T_2 values were produced for each hemisphere and each scan session. For each of the five hemispheres, the T_2 volumes from all scan sessions (including only brain tissue and excluding signals from the formaldehyde solution) were spatially normalized to the corresponding T_2 volume from the first session, using affine and

non-linear regularization with SPM5 (Wellcome Department of Imaging and Neuroscience, London, UK). Regions of interest (ROIs) were selected on the T_2 volumes at different locations within the brain, including in tissue near the surface (grey matter), as well as deep within the hemisphere (white matter) (Fig. 2). In selecting the ROIs, white matter lesions were avoided. Using the MNI template as a reference and the anterior commissure as the origin for a coordinate system with positive values in the right, anterior, and superior directions, respectively, a typical ROI near the surface was located at position [-31 -37 65] mm and a deep tissue ROI was located at [-31 -31 34] mm. A total of 11 ROIs were selected in each hemisphere and were propagated to all normalized T_2 volumes for that hemisphere. The mean T_2 value and its standard deviation were calculated for every ROI and all time-points. Linear regression was used to detect significant trends ($P < 0.05$) in the mean T_2 value of a given ROI over time. For each ROI, the mean T_2 values from all scan sessions were plotted as a function of time. Due to the shape of the resulting curves for deep tissue ROIs (see Results section), functions of the form $T_{2\text{est}} = A\exp(-c_1t) + B[1 - \exp(-c_2t)]$ were fitted to a deep-tissue T_2 time-course from each hemisphere using a least squares approach, where $T_{2\text{est}}$ was the estimated value of T_2 , and t was the postmortem time in days. Values for all four unknown parameters (A , B , c_1 , and c_2) were extracted and used to characterize the T_2 changes that occur in deep tissue of the hemispheres. Specifically, the times to minimum T_2 and to 95% of the asymptotic T_2 value were calculated for deep tissue ROIs.

T_2 difference maps were also produced by subtracting the absolute T_2 values of one scan session from those of an earlier session of the same hemisphere. The difference maps were presented in color-scale, with red in locations where T_2 values increased, blue where T_2 values decreased, and green where they remained approximately the same. These maps allowed assessment of T_2 changes between scan sessions throughout the hemispheres.

Simulations

A T_2 map from Hemisphere A was used to create a realistically shaped, 3-D model of a human cerebral hemisphere, which was treated as a homogeneous tissue mass with isotropic diffusion and a constant diffusion coefficient throughout. An infinite pool of 4% formaldehyde was assumed to form a boundary around the tissue at all times, and was allowed to diffuse into the tissue in a Fickian manner according to the following equation:

$$\frac{\partial [\text{CH}_2\text{O}]}{\partial t} = D\nabla^2 [\text{CH}_2\text{O}] \quad [1]$$

where brackets $[\cdot]$ indicate concentration at a given location, t is time, CH_2O is formaldehyde's molecular formula, and ∇^2 is the spatial Laplacian operator. The diffusion coefficient D was set to $8.0 \times 10^{-7} \text{ cm}^2\cdot\text{s}^{-1}$, which falls within the range of previously reported values (26,28-30). The concentration of formaldehyde was expressed as a unitless fraction, with a value of 1.0 corresponding to 4% solution. The diffusion simulation was carried out using a discretized version of Equation 1 with finite differences. Voxels measured $1.25 \times 1.25 \times 1.5 \text{ mm}^3$ and each timestep was 1.0 second long.

Initially, all tissue was classified as unfixed tissue (UT). During the simulation, UT was allowed to transform into either fixed tissue (FT) or decomposed tissue (DT). All concentrations of tissue were expressed as unitless fractions between zero and unity, and within each voxel the concentrations of UT , FT , and DT always summed to unity. In the transformation of UT to FT , it was assumed that two proteins become linked to each other via a formaldehyde-derived bridge (16-18,25,26) at a rate modeled by the following equation:

$$\text{rate} = k_1 [UT]^2 [\text{CH}_2\text{O}] \quad [2]$$

where the rate constant k_1 was assigned a value of $4.0 \times 10^{-6} \text{ s}^{-1}$, estimated from kinetic data of formaldehyde binding in rat kidney (25).

The decomposition of UT into DT was assumed to proceed only in the presence of an autolytic agent AA at a rate given by the following equation:

$$\text{rate} = k_2 [UT] [AA] \quad [3]$$

where k_2 is the rate constant. Equation 3 also describes the rate at which the model allows more AA to be released as decomposition proceeds, which leads to an increase in AA concentration. In the absence of any chemical fixation effects, this model would cause the decomposition process to follow a sigmoidal logistic curve similar to what has been observed in a previous study (27). The concentration of AA was expressed as a unitless fraction. Simulation of the decomposition process started from an initial AA concentration of 0.025 and the rate constant k_2 was set to $2.0 \times 10^{-6} \text{ s}^{-1}$.

Finally, T_2 values were calculated based on the relative concentrations of UT , FT , and DT within each voxel. In the present study, the extent of protein cross-linking in the non-decomposed portion of the intravoxel tissue was expressed as the fraction $C = FT / (UT + FT)$. Unfortunately, there is no data that explicitly defines the relationship between cross-linking and T_2 relaxation in brain tissue. In one study that investigated relaxation in polyacrylamide gels, R_2 values exhibited a complex biphasic dependence on cross-linking (19). In each phase, R_2 was proportional to the extent of protein cross-linking. There is good reason to believe that relaxation in brain tissue, which is much faster, does not exhibit this same biphasic dependence. Therefore, only one phase of that behavior was assumed:

$$T_{2,non-decomposed} = 20 + \frac{55}{1 + 12.5C} \quad [4]$$

Here, $T_{2,non-decomposed}$ was constrained at the extreme values of C by reasonable values of T_2 for unfixed postmortem tissue (75 ms) and fully fixed tissue (24 ms). Other functional forms are possible and may yield quantitatively different simulation results. However, Equation 4 reasonably captures the nature of the available data.

The decomposed tissue fraction was assigned a relatively high $T_{2,decomposed}$ value of 150.0 ms. The total signal decay in each voxel was modeled as a sum of the exponential decays from the decomposed and non-decomposed tissue, weighted by their respective partial volumes. The simulated T_2 measurement was thus extracted according to the following equation:

$$T_{2,simulated} = \frac{-t}{\ln \left[(UT+FT) \cdot \exp\left(-t/T_{2,non-decomposed}\right) + DT \cdot \exp\left(-t/T_{2,decomposed}\right) \right]} \quad [5]$$

where t is the decay time and the initial signal was assumed to equal unity.

Results

Experiments

The T_2 values of ROIs selected near the surface of the hemispheres remained almost constant during the six months of this study (Fig. 3). Linear regression confirmed that no significant positive or negative trends existed over the course of six months of scanning. Any changes that occurred from week to week were apparently random and occurred at arbitrary times postmortem. In general, the T_2 relaxation times of ROIs near the surface fluctuated around a value of approximately 50 ms.

ROIs selected in deep tissue of each hemisphere initially exhibited a rapid reduction in T_2 values from about 55 ms to 30 ms in a 14-day period, and then a gradual increase to a plateau of approximately 40 ms (Fig. 3). The initial sharp decrease was present in all five hemispheres, and the subsequent gradual increase was significant in four out of five hemispheres ($P < 0.001$), with Hemisphere B only showing a non-significant tendency to increase. Curves of the form $T_{2\text{est}} = A\exp(-c_1t) + B[1 - \exp(-c_2t)]$ were fitted to the deep tissue data from all five hemispheres (Fig. 3). The parameters A , B , c_1 , and c_2 , along with the time postmortem to reach the minimum T_2 value, and the time to reach 95 percent of the asymptotic T_2 value, were calculated based on these curves (Table 2). The mean time postmortem to reach the minimum T_2 value was 32 days, ranging from 20 to 46 days among the five hemispheres. The mean time to reach 95 percent of the asymptotic T_2 value was 77 days, ranging from 48 to 96 days. Similar results were obtained for different near surface and deep tissue ROIs than the ones for which results are shown.

The T_2 difference maps in Fig. 4 show areas where T_2 values increased or decreased between selected time-points. These time-points were as follows: Hemisphere A, 13, 27, 76, and 174 days postmortem; Hemisphere B, 13, 34, 90, and 174 days postmortem; Hemisphere C, 12, 26, 68, and 173 days postmortem; Hemisphere D, 3, 17, 59, and 164 days postmortem; and Hemisphere E, 5, 33, 75, and 159 days postmortem. Over the first few weeks, T_2 values decreased over the inner portions of the formaldehyde-fixed hemispheres, while T_2 values increased in some small regions near the surface of the hemispheres. Over the next several weeks, each hemisphere exhibited widespread T_2 increase concentrated toward the middle of the hemispheres. Finally, in the last several scan sessions, a span of more than three months, the T_2 values remained relatively stable throughout the hemispheres.

Simulations

Near the edge of the model hemisphere, T_2 values decreased rapidly to a value of approximately 26 ms (Fig. 5). This decrease occurred within approximately 3 days postmortem (21), depending on the exact depth of the tissue. Following the initial decrease, T_2 values of edge voxels remained approximately constant, increasing by less than 1 ms over the next 100 days.

In a typical deep tissue voxel, T_2 underwent a rapid decrease to approximately 38 ms over the period from 2 days to 16 days postmortem (Fig. 5). Subsequently, the T_2 gradually increased to a final value of 49 ms. As shown in Table 2, 37 days postmortem were required for the T_2 to reach 95 percent of this value. T_2 changes throughout one sagittal slice of the simulated brain are shown in Fig. 6. The T_2 changes in deep and near surface tissue can be explained by the values of UT , FT , and DT over time, as shown in Fig. 7.

Discussion

Chemical fixation of a postmortem human brain hemisphere alters the tissue's MR properties over time. Furthermore, the fixative agent gradually diffuses inward from the surface of the brain, causing the effects of fixation to be dependent not only on time, but also on position within the sample. Characterization of these effects is critical for correct interpretation of postmortem MRI results. Therefore, this study aimed to investigate longitudinally T_2 relaxation changes occurring in postmortem human brain hemispheres during formaldehyde fixation.

The results of the current investigation suggest that upon immersion of a brain hemisphere in fixative solution, the effects of fixation occur rapidly near the surface of the brain compared to deep tissue. By the time the first postmortem scan was conducted for any of the hemispheres in this study, the T_2 values near the surface of the hemispheres had already decreased to a plateau of approximately 50 ms. Although the decrease was not captured in these experiments, the *in vivo* value for cortical grey matter is known to be approximately 100 ms at 3T (30). The decrease was apparently due to formaldehyde-induced protein cross-linking, which increases tissue rigidity and decreases T_2 values. These results suggest that the process of fixation and its effects on T_2 values of near-surface brain tissue are completed relatively rapidly, occurring within a few days of immersion in formaldehyde solution. This finding is in agreement with previously published studies (20-22) and also with the results of simulations carried out as part of the current study.

In some cases, substantial T_2 changes existed between consecutive scan sessions near the surface of the hemispheres. However, these changes were not part of a consistent trend for any given brain, and there was no recognizable trend among brains. Positive and negative fluctuations in the T_2 values near the surface of the hemispheres were likely the result of errors in the normalization process that caused the ROIs to be slightly dislocated between sessions.

In deep tissue, a reduction in the T_2 values was observed in the first 20 days postmortem, in all five hemispheres. This decrease was presumably due to the formaldehyde reaching and gradually fixing that tissue. The fact that the decrease in T_2 values was slower in deep tissue compared to tissue near the surface of the hemispheres may be due to the fact that a longer period of time is required for formaldehyde to diffuse to the middle portions of the brain and accumulate in sufficient quantities to cause complete fixation. In a 1941 study (27), 30 hours were required for 4% formaldehyde solution to penetrate 30 millimeters into coagulated chicken plasma. In a 1960 study (28) it was claimed that three days are required for the same solution to penetrate 30 millimeters into rabbit liver tissue. Recent findings suggest that approximately 124 days are required for 4% formaldehyde to penetrate 30 millimeters into whole human spleens (29). Another study found that 62 days are required for 30 mm of penetration into mammalian liver tissue (31). To our knowledge, this is the first study to report that at least 20 days are required for a sufficient amount of formaldehyde to diffuse to the innermost portions of a human brain hemisphere to cause fixation (Fig. 3).

Following the initial decrease of T_2 values in deep tissue of the hemispheres, a gradual increase of T_2 values was measured over the next one to two months. This behavior was shown to be statistically significant in four out of the five hemispheres, using linear regression through the points between the minimum T_2 measurement and the T_2 measurement at the end of the gradual rise (60 to 90 days postmortem). One possible factor that may have led to this latent increase in T_2 is the fact that, compared to tissue near the surface of the hemisphere, fixation of deep tissue is delayed due to distance from the surface, as well as due to consumption of the fixative agent in more superficial layers of

tissue. Thus, decomposition progresses in deep tissue even after fixation is completed in regions near the surface of the hemispheres. This decomposition increases the water content of deep tissue, thereby elevating T_2 values. The simulation results support this hypothesis.

There are a number of reasons why the latent T_2 increase observed in the current study has not been reported previously. First, in this work, T_2 values were measured at deep locations within the hemispheres, while other studies focused primarily on tissue near the surface of the brain, with the deepest ROI at approximately 1.4 cm from the surface (21). Fixation in that location was probably completed rather quickly, thereby not allowing the T_2 increase. Second, the current work included data points from up to six months postmortem, while most other studies conducted MR scans for only about one month postmortem. However, most of the T_2 increase that was observed in this study was seen later than one month postmortem. Finally, the T_2 behavior in question may have been influenced by factors such as the temperature of the hemispheres while in storage, the time interval between death and immersion in formaldehyde, and preparation of the formaldehyde solution (stock formalin versus preparation from paraformaldehyde), among others.

In deep tissue, after the gradual T_2 increase, a plateau was reached for all hemispheres by approximately three months postmortem. The T_2 value of deep tissue at the plateau was lower than that of tissue near the surface of the hemispheres. This was likely due to the fact that the deep tissue ROI was selected in white matter, while the ROI near the surface of the hemisphere contained grey matter (higher T_2 than white matter). In simulations, however, no distinction was made between regions of white and grey matter, and this is why the simulations showed the near surface T_2 plateau to be slightly lower than the deep tissue T_2 plateau.

The exponential model used to describe the experimental T_2 behavior of deep tissue through time postmortem fit the data reasonably well ($R^2 > 0.95$ for all five hemispheres). However, it should be emphasized that this model was purely empirical. Physical processes, such as those accounted for in the simulations, were only modeled phenomenologically. In addition, the proposed model was tested only for the period of time studied in this investigation. No measurements were obtained within three days postmortem, and thus the model has not been tested for that time interval. There is actually an indication that the empirical model does not accurately describe the behavior of T_2 values immediately after death and immersion of the hemisphere in formaldehyde solution, since for zero days postmortem the model provides T_2 values in excess of 200 ms for some hemispheres, which are significantly higher than those in normal living tissue.

T_2 values were measured in this work using only two different TEs and assuming mono-exponential T_2 decay. Although the most unbiased estimate of T_2 relaxation times can be achieved with a large number of TEs (32), our approach was sensitive to the significant T_2 changes due to fixation and decomposition, and allowed for a short total scan time. In future work, it may be worthwhile to assume multi-exponential T_2 decay (33,34) and, using multiple echoes, perform a multi-compartment analysis of T_2 relaxation as a function of time postmortem, in order to investigate the T_2 changes in different water environments during fixation.

To our knowledge, no previous studies have simulated diffusion of formaldehyde into tissue, consumption of formaldehyde during fixation, and tissue decomposition. Therefore, assumptions had to be made in the selection of appropriate model parameters. Although each part of our model was based on experimental results from previous studies, and great care was taken to make the assumptions reasonable, further investigation is required for validation of the parameter values and the model as a whole.

Two notable assumptions were made in order to simplify the simulations carried out in this study. First, the brain hemisphere was treated as a homogeneous mass with isotropic diffusion and a constant diffusion coefficient throughout. No distinction was made between the differences in the tissue properties of white and grey matter at different locations throughout the specimen. Second, the process of formaldehyde-induced protein cross-linking was assumed to occur in one step that was second order with respect to the concentration of unfixed protein. However, others have shown that cross-linking itself occurs in two separate steps, with formaldehyde reacting first with one protein and then with another to form a methylene bridge between the two (17,18,26). Nevertheless, the one-step assumption reduced the complexity of the model without sacrificing agreement with experimental kinetic data (25). Despite these two major assumptions, simulations revealed the possible mechanisms behind T_2 changes that occur postmortem during formaldehyde fixation.

The interest of the MR community in imaging postmortem brain tissue has increased significantly over the past few years. The recent development of MR imaging tools that can provide information about the microstructure of brain tissue has inspired researchers to image postmortem brain tissue in order to develop techniques for virtual non-invasive histology, and maps of brain connections with very high spatial resolution. MRI of postmortem brain tissue may also be used for “proof of concept” studies, where an imaging technique is applied on postmortem brain tissue, and the results are compared to histological findings in order to test the diagnostic value of the technique. However, it is extremely crucial to first understand the changes in the MRI properties of brain tissue postmortem and in combination with fixation using formaldehyde. The current work addressed exactly that issue, namely provided longitudinal information on T_2 relaxation changes occurring in human brain hemispheres during formaldehyde fixation. These findings can possibly be extended to postmortem whole brain as long as the medial surface of each hemisphere is exposed to formaldehyde. In contrast, the results of this study cannot be extended to investigations on sectioned human brain, whole brains that have been infused with fixative agent prior to death, or small animal brains, since in these cases, even deep tissue is easily reached by the fixative.

Conclusions

This study demonstrated that, during fixation, the T_2 relaxation properties of human brain hemispheres depend on both fixation time and position within the hemisphere. Specifically, when a brain hemisphere is immersed in fixative solution shortly after death, the T_2 values near the surface of the hemisphere decrease sharply within the first days postmortem and remain approximately constant thereafter. Thus, the effects of decomposition and fixation on T_2 values are relatively rapid in regions near the surface of a human brain hemisphere. Conversely, up to approximately 46 days may be required for the T_2 values of deep tissue to reach a minimum. The delay in the T_2 decrease in deep tissue compared to tissue near the surface of a hemisphere suggests that a relatively long period of time is required for formaldehyde to diffuse to deep tissue in sufficient quantity to cause substantial protein cross-linking. Furthermore, after the minimum is reached, and over the following one to two months, the deep tissue T_2 values gradually increase, eventually reaching a plateau. This gradual T_2 increase may indicate that even after some cross-linking has occurred in deep tissue, its water content increases, counteracting the T_2 reduction due to protein cross-linking. Finally, this study also demonstrated that the T_2 values in all parts of the five formaldehyde-fixed human brain hemispheres that were examined, stabilized (reached 95% of their plateau) within 96 days postmortem.

Acknowledgments

The authors thank Dr. Minzhi Gui and Ashish Tamhane, for their help in conducting MR scans; Veronica Flores and Karen Skish, for preparing the brain hemispheres; Dr. Robert B. Dawe, for his help in the design and construction of the anti-vibration bridge, and Dr. Georgia Papavasiliou, for her help in the development of the decomposition-diffusion-fixation model. We also thank the participants in the Rush Memory and Aging Project, Religious Orders Study, and Clinical Core of the Rush Alzheimer's Disease Center. This work was supported by Academic Rewards for College Scientists, Inc. (Chicago Chapter), and also by NIA grants P30 AG10161, R01 AG15819, and R01 AG17917.

References

1. Bobinski M, de Leon MJ, Wegiel J, Desanti S, Convit A, Saint Louis LA, Rusinek H, Wisniewski HM. The histological validation of post mortem magnetic resonance imaging-determined hippocampal volume in Alzheimer's disease. *Neuroscience*. 2000; 95:721–725. [PubMed: 10670438]
2. Larsson E, Englund E, Sjöbeck M, Lätt J, Brockstedt S. MRI with diffusion tensor imaging post-mortem at 3.0 T in a patient with frontotemporal dementia. *Dement Geriatr Cogn Disord*. 2004; 17:316–319. [PubMed: 15178944]
3. Fazekas F, Kleinert R, Roob G, Kleinert G, Kapeller P, Schmidt R, Hartung H. Histopathologic analysis of foci of signal loss on gradient-echo T_2^* -weighted MR images in patients with spontaneous intracerebral hemorrhage: evidence of microangiopathy-related microbleeds. *Am J Neuroradiol*. 1999; 20:637–642. [PubMed: 10319975]
4. Fernando MS, O'Brien JT, Perry RH, English P, Forster G, McMeekin W, Slade JY, Golkhar A, Matthews FE, Barbert R, Kalaria RN, Ince PG. Comparison of the pathology of cerebral white matter with post-mortem magnetic resonance imaging (MRI) in the elderly brain. *Neuropath Appl Neuro*. 2004; 30:385–395.
5. Bronge L, Bogdanovic N, Wahlund L. Postmortem MRI and histopathology of white matter changes in Alzheimer brains. *Dement Geriatr Cogn Disord*. 2002; 13:205–212. [PubMed: 12006730]
6. Everall IP, Chong WK, Wilkinson ID, Paley MN, Chinn RJ, Hall-Craggs MA, Scaravilli F, Lantos PL, Luthert PJ, Harrison MJ. Correlation of MRI and neuropathology in AIDS. *J Neurol Neurosurg Ps*. 1997; 62:92–95.
7. Moore GR, Leung E, MacKay AL, Vavasour IM, Whittall KP, Cover KS, Li DK, Hashimoto SA, Oger J, Sprinkle TJ, Paty DW. *Neurology*. 2000; 55:1506–1510. [PubMed: 11094105]
8. Newcombe J, Hawkins CP, Henderson CL, Patel HA, Woodroffe MN, Hayes GM, Cuzner ML, MacManus D, du Boulay EP, McDonald WI. Histopathology of multiple sclerosis lesions detected by magnetic resonance imaging in unfixed postmortem central nervous system tissue. *Brain*. 1991; 114:1013–1023. [PubMed: 2043938]
9. van Walderveen MA, Kamphorst W, Scheltens P, van Waesberghe JH, Ravid R, Valk J, Polman CH, Barkhof F. Histopathologic correlate of hypointense lesions on T_1 -weighted spin-echo MRI in multiple sclerosis. *Neurology*. 1998; 50:1282–1288. [PubMed: 9595975]
10. Awad IA, Johnson PC, Spetzler RF, Hodak JA. Incidental subcortical lesions identified on magnetic resonance imaging in the elderly. II. Postmortem pathological correlations. *Stroke*. 1986; 17:1090–1097. [PubMed: 3810706]
11. Braffman BH, Zimmerman RA, Trojanowski JQ, Gonatas NK, Hickey WF, Schlaepfer WW. Brain MR: pathologic correlation with gross and histopathology. 1. Lacunar infarction and Virchow-Robin spaces. *Am J Neuroradiol*. 1988; 151:551–558.
12. Braffman BH, Zimmerman RA, Trojanowski JQ, Gonatas NK, Hickey WF, Schlaepfer WW. Brain MR: pathologic correlation with gross and histopathology. 2. Hyperintense white-matter foci in the elderly. *Am J Neuroradiol*. 1988; 151:559–566.
13. House MJ, St. Pierre TG, Kowdley KV, Montine T, Connor J, Beard J, Berger J, Siddaiah N, Shankland E, Jin L. Correlation of proton transverse relaxation rates (R_2) with iron concentrations in postmortem brain tissue from Alzheimer's disease patients. *Magn Reson Med*. 2007; 57:172–180. [PubMed: 17191232]
14. Thickman DI, Kundel HL, Wolf G. Nuclear magnetic resonance characteristics of fresh and fixed tissue: the effect of elapsed time. *Radiology*. 1983; 148:183–185. [PubMed: 6856832]

15. D'Arceuil H, de Crespigny A. The effects of brain tissue decomposition on diffusion tensor imaging and tractography. *NeuroImage*. 2007; 36:64–68. [PubMed: 17433879]
16. Fishbein KW, Gluzband YA, Kaku M, Ambia-Sobham H, Shapses SA, Yamauchi M, Spencer RG. Effects of formalin fixation and collagen cross-linking on T_2 and magnetization transfer in bovine nasal cartilage. *Magn Reson Med*. 2007; 57:1000–1011. [PubMed: 17534923]
17. Metz B, Kersten GF, Hoogerhout P, Brugghe HF, Timmermans HA, de Jong A, Meiring H, ten Hove J, Hennink WE, Crommelin DJ, Jiskoot W. Identification of formaldehyde-induced modifications in proteins: reactions with model peptides. *J Biol Chem*. 2004; 279:6235–6243. [PubMed: 14638685]
18. Puchtler H, Meloan SN. On the chemistry of formaldehyde fixation and its effects on immunohistochemical reactions. *Histochemistry*. 1985; 82:201–204. [PubMed: 3997553]
19. Kennan RP, Richardson KA, Zhong J, Maryanski MJ, Gore JC. The effects of cross-link density and chemical exchange on magnetization transfer in polyacrylamide gels. *J Magn Reson B*. 1996; 110:267–277. [PubMed: 8867442]
20. Blamire AM, Rowe JG, Styles P, McDonald B. Optimising imaging parameters for post mortem MR imaging of the human brain. *Acta Radiol*. 1999; 40:593–597. [PubMed: 10598845]
21. Yong-Hing CJ, Obenaus A, Stryker R, Tong K, Sarty GE. Magnetic resonance imaging and mathematical modeling of progressive formalin fixation of the human brain. *Magn Reson Med*. 2005; 54:324–332. [PubMed: 16032673]
22. Tovi M, Ericsson A. Measurements of T_1 and T_2 over time in formalin-fixed human whole-brain specimens. *Acta Radiol*. 1992; 33:400–404. [PubMed: 1389643]
23. Pfefferbaum A, Sullivan EV, Adalsteinsson E, Garrick T, Harper C. Postmortem MR imaging of formalin-fixed human brain. *NeuroImage*. 2004; 21:1585–1595. [PubMed: 15050582]
24. Bennett DA, Schneider JA, Aggarwal NT, Arvanitakis Z, Shah R, Kelly JF, Fox JH, Cochran EJ, Arends D, Treinkman A, Wilson RS. Prediction rules guiding the clinical diagnosis of Alzheimer's disease in two community-based cohort compared to standard practice in a clinic-based cohort study. *Neuroepidemiology*. 2006; 27:169–176. [PubMed: 17035694]
25. Fox CH, Johnson FB, Whiting J, Roller PP. Formaldehyde fixation. *J Histochem Cytochem*. 1985; 33:845–853. [PubMed: 3894502]
26. Baker, JR. The reactions of fixatives with proteins. 1. The visible effects. In: Baker, JR., editor. *Principles of biological microtechnique*. New York: Wiley; 1958. p. 31-43.
27. Carter DO, Yellowlees D, Tibbett M. Cadaver decomposition in terrestrial ecosystems. *Naturwissenschaften*. 2007; 94:12–24. [PubMed: 17091303]
28. Medawar PB. The rate of penetration of fixatives. *J Roy Microsc Soc*. 1941; 61:46–57.
29. Dempster WT. Rates of penetration of fixing fluids. *Am J Anat*. 1960; 107:59–72. [PubMed: 13721811]
30. Start RD, Layton CM, Cross SS, Smith JH. Reassessment of the rate of fixative diffusion. *J Clin Pathol*. 1992; 45:1120–1121. [PubMed: 1479044]
31. Baker, JR. Primary fixatives considered separately 2. Non-coagulants. In: Baker, JR., editor. *Principles of biological microtechnique*. New York: Wiley; 1958. p. 31-43.
32. Wansapura JP, Holland SK, Dunn RS, Ball WS. NMR relaxation times in the human brain at 3.0 tesla. *J Magn Reson Im*. 1999; 9:531–538.
33. House MJ, St. Pierre TG, Foster JK, Martins RN, Clarnette R. Quantitative MR imaging R2 relaxometry in elderly participants reporting memory loss. *AJNR Am J Neuroradiol*. 2006; 27:430–439. [PubMed: 16484425]
34. MacKay A, Whittall K, Adler J, Li D, Paty D, Graeb D. In vivo visualization of myelin water in brain by magnetic resonance. *Magn Reson Med*. 1994; 31:673–7. [PubMed: 8057820]
35. Du YP, Chu R, Hwang D, Brown MS, Kleinschmidt-Demasters BK, Singel D, Simon JH. Fast multislice mapping of the myelin water fraction using multicompartement analysis of T_2^* decay at 3T: a preliminary postmortem study. *Magn Reson Med*. 2007; 58:865–870. [PubMed: 17969125]

List of Symbols

S₁	Italic upper case 'ess', subscript Roman 'one'
S₂	Italic upper case 'ess', subscript Roman 'two'
t	Italic lower case 'tee'
TE₁	Italic upper case 'tee', italic upper case 'ee', subscript Roman 'one'
TE₂	Italic upper case 'tee', italic upper case 'ee', subscript Roman 'two'
P	Italic upper case 'pee'
A	Italic upper case 'ay'
B	Italic upper case 'bee'
c₁	Italic lower case 'see', subscript Roman 'one'
c₂	Italic lower case 'see', subscript Roman 'two'
D	Italic upper case 'dee'
UT	Italic uppercase 'you', italic uppercase 'tee'
k₁	Italic lower case 'kay', subscript Roman 'one'
FT	Italic upper case 'eff', italic upper case 'tee'
AA	Italic upper case 'ay', italic upper case 'ay'
k₂	Italic lower case 'kay', subscript Roman 'two'
DT	Italic upper case 'dee', italic upper case 'tee'
C	Italic upper case 'see'
K	Italic upper case 'kay'
R²	Italic upper case 'ar', superscript 'two'

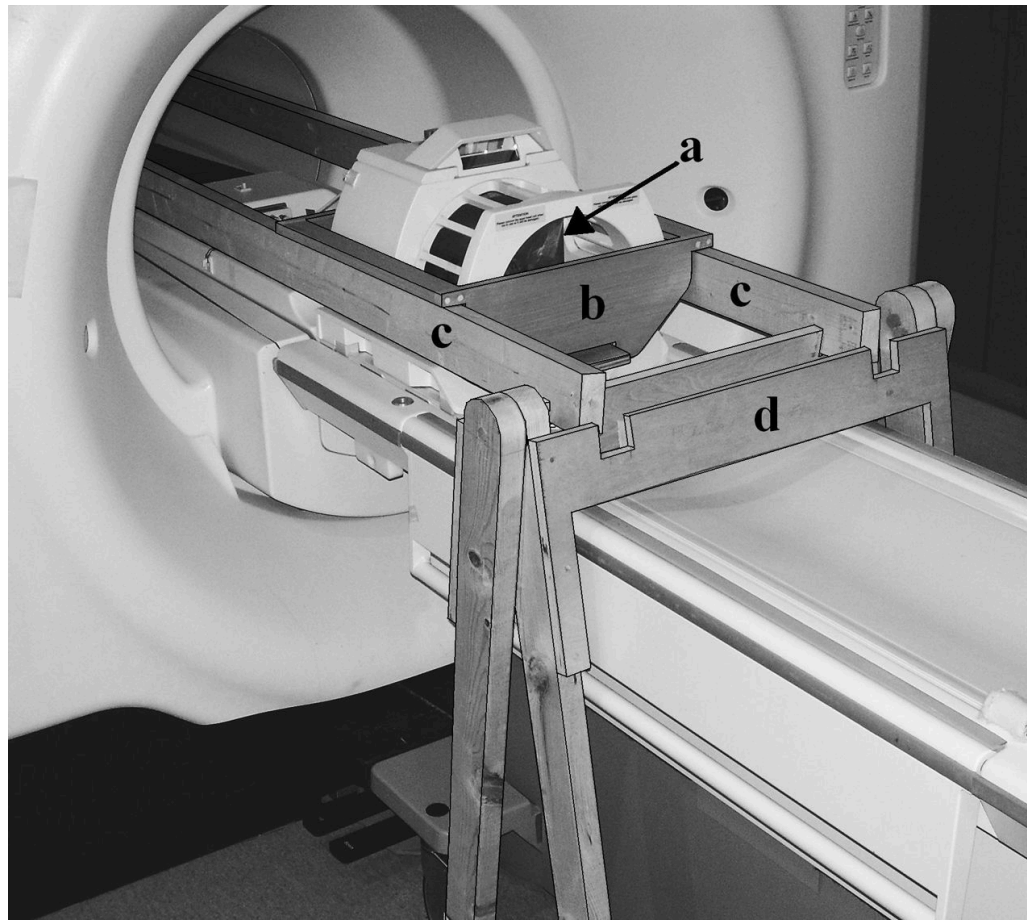


Figure 1.

The wooden bridge-like apparatus (outlined for clarity) that was used to suspend the brain hemispheres within the scanner, in order to reduce vibration of the specimen. The hemisphere, in its plastic container (a), was placed in the cradle (b). The cradle was suspended from two long beams (c) that ran through the bore of the magnet and were supported by frames (d) on both ends. The entire structure contained no metal and made no direct contact with the scanner.

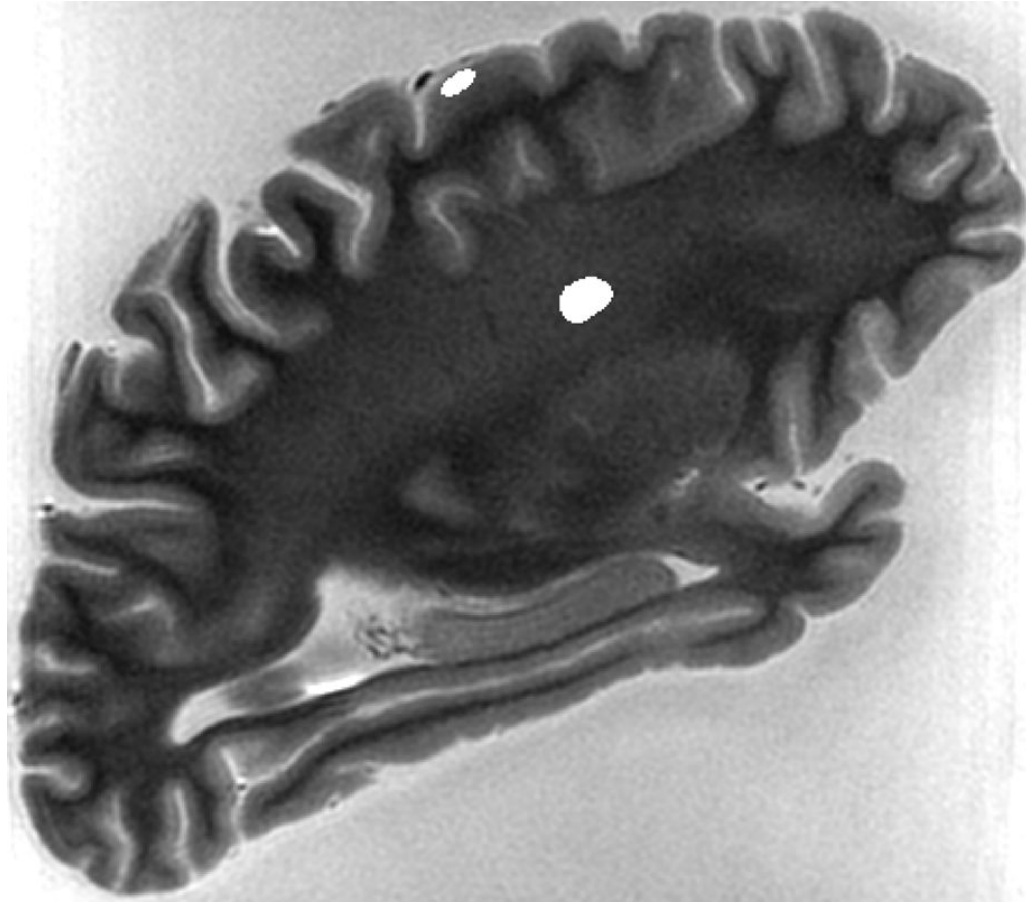


Figure 2.
Typical ROIs selected in deep white matter (colored grey) and in grey matter near the surface of the brain (colored white).

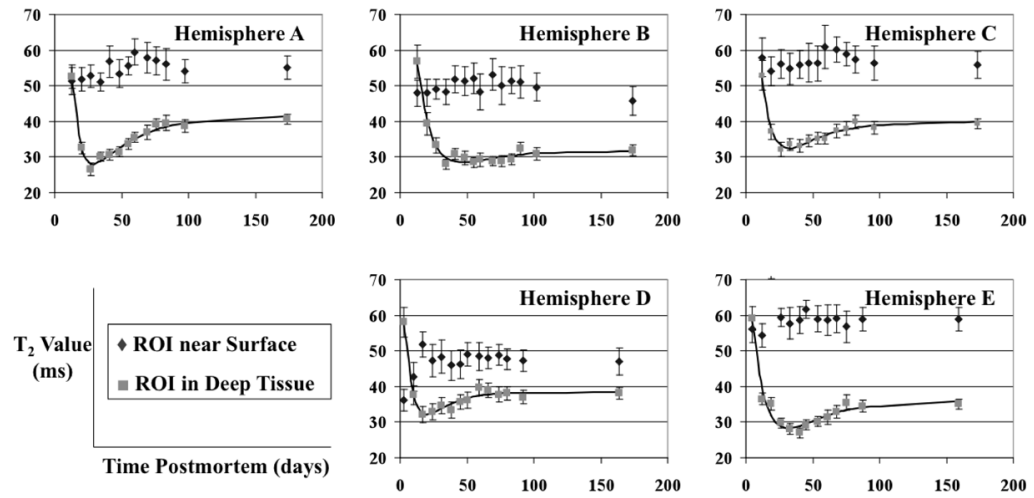


Figure 3.

T_2 values in ROIs near the surface of the hemispheres (◆) and in deep tissue (■), plotted over time, for all five brain hemispheres. The solid lines represent the behavior of T_2 values in deep tissue as modeled by the function $T_{2\text{est}} = A\exp(-c_1t) + B[1 - \exp(-c_2t)]$. The error-bars show the standard deviation of the measurements.

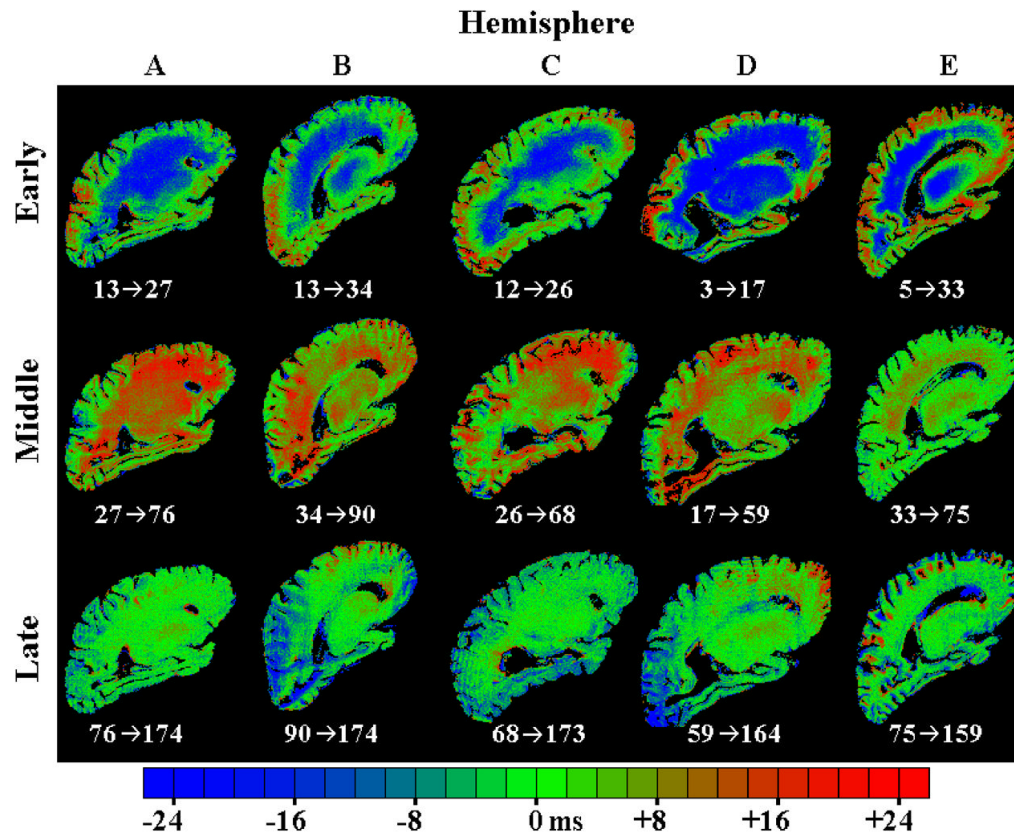


Figure 4.

T_2 difference maps for all five hemispheres, showing the changes in T_2 that occur during three different postmortem time periods. The early phase is defined as the time over which T_2 decreased in deep tissue of each hemisphere. The middle phase corresponds to the subsequent gradual rise in T_2 values of deep tissue over the next one to two months, and the late phase corresponds to the T_2 plateau that was reached two to three months postmortem. The numbers below each image indicate the time points (in days postmortem) that were compared in order to generate that image.

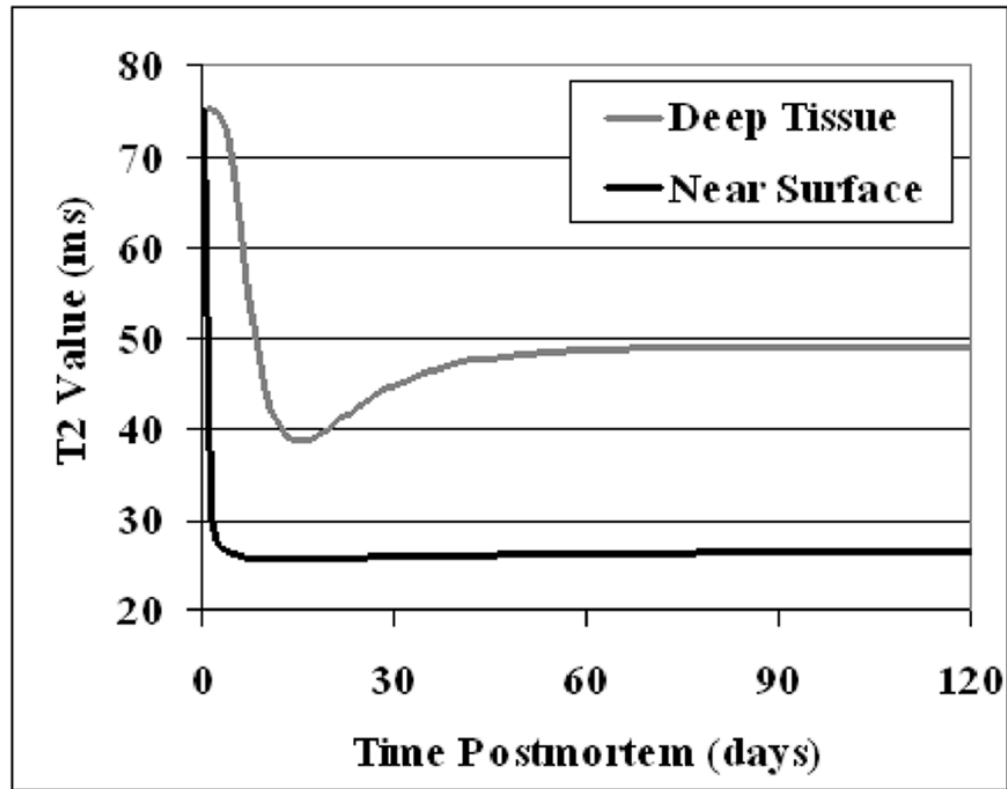


Figure 5. Simulated T_2 values in voxels near the surface of the 3-D model hemisphere (black curve) and in deep tissue (grey curve), plotted over time.

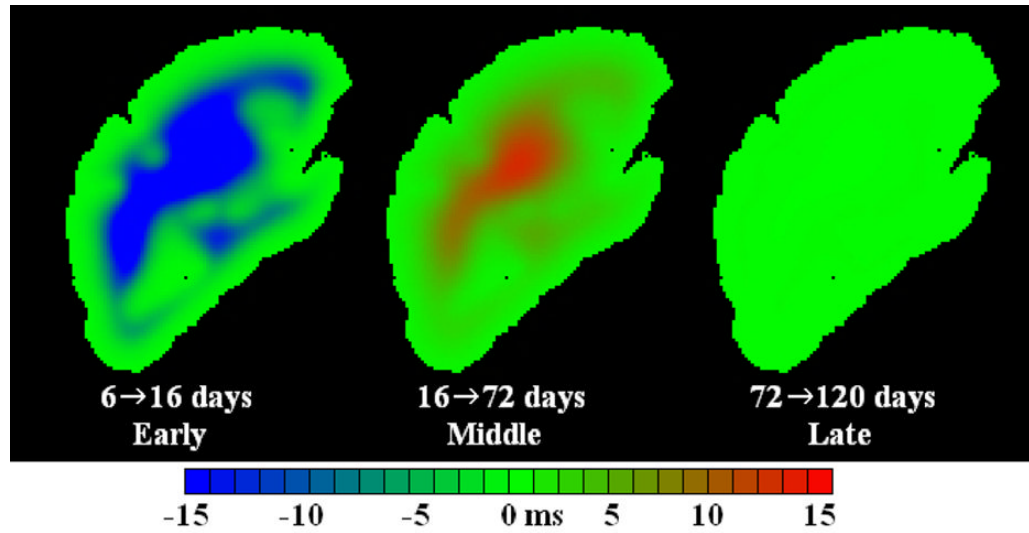


Figure 6. T_2 difference maps generated by numerical simulation of the fixation process. Simulated difference maps are analogous to those obtained in the actual experiments shown in Fig. 4.

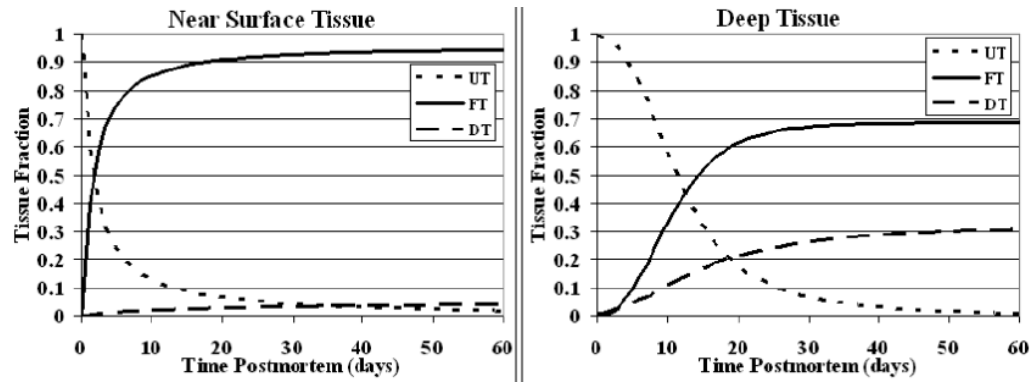


Figure 7. Simulated changes in unfixed tissue (*UT*), fixed tissue (*FT*), and decomposed tissue (*DT*) fractions at deep and near surface locations in the model hemisphere over time. The sum of all three tissue fractions is equal to unity at every point in time for both locations.

Table 1

Subject details.

Subject	Left or Right Hemisphere	Postmortem Interval	Age at Death	Sex
A	R	4.8 hours	88.1 years	F
B	R	3.3	78.0	F
C	R	4.0	84.9	M
D	L	5.0	92.2	M
E	L	5.9	76.3	M
Mean \pm S.D.	--	4.6 \pm 1.0	83.9 \pm 6.71	--

Table 2

T_2 behavior in deep tissue of the hemispheres: Results from actual experiments and simulations.

Hemisphere	Time to Minimum T_2	Time to Stable T_2	Asymptotic T_2 Value
A	29 days	96 days	41.5 ms
B	46	77	31.7
C	32	78	39.9
D	20	48	38.4
E	32	88	36.0
Mean \pm S.D.	32 ± 9	77 ± 18	37.5 ± 3.8
Simulation	16	37	49.0 ms